

Institute of Veterinary Pathology  
of the Vetsuisse Faculty, University of Zurich

Director: Prof. Dr. med. vet. Anja Kipar

Work under the academic supervision of  
Prof. Dr. med. vet. Anja Kipar

**Canine Dilated Cardiomyopathy: Diffuse Remodeling, Focal Lesions and the  
Involvement of Macrophages and New Vessel Formation**

**Inaugural Thesis**

to obtain the title of Doctor from the  
Vetsuisse Faculty University of Zurich

submitted by

**Stefania Gasparini**

Veterinarian  
Padova, Italy

Approved at the request of

Prof. Dr. med. vet. Anja Kipar, Supervisor  
Prof. Dr. med. vet. Tony Glaus, Co-supervisor

**2019**



## TABLE OF CONTENTS

1. Abstract	<u>4</u>
2. Summary	<u>5</u>
3. Manuscript	<u>6-51</u>
4. Curriculum vitae	

Vetsuisse Faculty University of Zurich 2019

Stefania Gasparini

Institute of Veterinary Pathology  
ivpz@vetpath.uzh.ch

Canine dilated cardiomyopathy: diffuse remodeling, focal lesions and the involvement of macrophages and new vessel formation

Dilated cardiomyopathy (DCM) is one of the most common cardiac diseases of dogs. A detailed understanding of the disease process is still lacking, but myocardial inflammation and fibrosis are suspected to contribute. This study aimed to gain information on the pathogenesis of canine DCM, by evaluating myocardial histological changes alongside the transcription of remodelling markers. The myocardium of 17 dogs with DCM and 6 control dogs was examined by histology, immunohistology, morphometry and reverse transcription-quantitative PCR. DCM hearts exhibited relatively subtle, but statistically significant diffuse quantitative changes: an increase in interstitial macrophages and interstitial fibrosis, and a reduced proportion of contractile tissue. These changes were associated with a significantly higher myocardial transcription of remodelling enzymes, cytokines and intracellular adhesion molecule (ICAM)-1. In addition to the diffuse changes, focal cell-rich lesions were observed. These comprised infiltrating macrophages, new vessels and fibrosis and were associated with cardiomyocyte degeneration. Both macrophages and cardiomyocytes were found to express functional markers, such as transforming growth factor- $\beta$  and vascular endothelial growth factor. The present findings confirm that DCM hearts undergo diffuse myocardial remodelling processes to which both cardiomyocytes and macrophages might actively contribute.

Keywords: dilated cardiomyopathy, dogs, histology, fibrosis, macrophages

Stefania Gasparini

Institute of Veterinary Pathology  
ivpz@vetpath.uzh.ch

Kanine dilatative Kardiomyopathie: diffuse Umbauprozesse, herdförmige Veränderungen und die Beteiligung von Makrophagen und der Bildung neuer Blutgefässe

Die dilatative Kardiomyopathie (DCM) ist eine der häufigsten Herzerkrankungen des Hundes. Bis jetzt ist das Wissen zur Entstehung dieser Erkrankung begrenzt, es wird jedoch davon ausgegangen, dass Entzündung und Fibrose daran beteiligt sind. Das Ziel der vorgelegten Arbeit war es, durch detaillierte histologische und molekulare Untersuchungen zur Transkription von "Remodelling"-Markern Informationen zur Pathogenese der kaninen DCM zu erhalten. Es wurden Herzen von 17 Hunden mit DCM und 6 Kontrollhunden mittels Histologie, Immunhistologie, Morphometrie und quantitativer RT-PCR untersucht. Das DCM-Myokardium wies recht unauffällige, jedoch statistisch signifikante quantitative Veränderungen auf: eine erhöhte Zahl an Makrophagen im Interstitium, eine vermehrte interstitielle Fibrose sowie eine Verminderung des Anteils an kontraktilen Gewebe. Damit verbunden war eine signifikant erhöhte Transkription von Remodelling-Enzymen, Zytokinen und dem intracellular adhesion molecule (ICAM)-1. Ausserdem fanden sich teils mehrere zellreiche Herde mit infiltrierenden Makrophagen, neuen Gefässen und Fibrose sowie vereinzelt degenerierenden Kardiomyozyten. Sowohl Makrophagen als auch Kardiomyozyten zeigten eine Expression funktionaler Marker wie transforming growth factor- $\beta$  und vascular endothelial growth factor. Die Ergebnisse der Studie bestätigen, dass DCM mit diffusen Umbauprozessen im Myokardium einhergeht, zu denen Kardiomyozyten und Makrophagen aktiv beizutragen scheinen.

Canine dilated cardiomyopathy: diffuse remodeling, focal lesions and the involvement of macrophages and new vessel formation

**S. Gasparini<sup>1\*</sup>, S. Fonfara<sup>2</sup>, S. Kitz<sup>1</sup>, U. Hetzel<sup>1</sup>, A. Kipar<sup>1</sup>**

The Veterinary Cardiac Pathophysiology Consortium, <sup>1</sup>Institute of Veterinary Pathology, Vetsuisse Faculty, University of Zurich, Switzerland; <sup>2</sup>Department of Clinical Studies, Ontario Veterinary College, University of Guelph, Canada

\* Author's present address:

San Marco Veterinary Laboratory, Via dell'Industria 3, 35030, Veggiano (Pd), Italy

**Corresponding Author:**

Anja Kipar

Institute of Veterinary Pathology

Vetsuisse Faculty

University of Zurich

Winterthurerstrasse 268

8057 Zurich

Switzerland

Email: [anja.kipar@uzh.ch](mailto:anja.kipar@uzh.ch)

## **Abstract**

Dilated cardiomyopathy (DCM) is among the most common cardiac diseases in dogs. Its pathogenesis is not yet fully understood, but myocardial remodeling and inflammation are suspected to be involved. The present study aimed to characterize the pathological processes in canine DCM, investigating morphological changes in association with the expression of relevant cytokines and remodeling markers. The myocardium of 17 dogs with DCM and 6 dogs without cardiac diseases was histologically evaluated, and selected cases were further examined by immunohistology, morphometry and reverse transcription-quantitative PCR. In DCM, the myocardium exhibited subtle, though statistically significant diffuse quantitative changes. These comprised increased interstitial collagen deposition and macrophage numbers, and an overall reduced proportion of contractile tissue. This was accompanied by a significant increase in myocardial transcription of intracellular adhesion molecule (ICAM)-1, inflammatory cytokines and remodeling enzymes. Laser microdissection showed that cardiomyocytes transcribed most relevant markers. In addition, multifocal cell-rich lesions, characterized by fibrosis, neovascularization, macrophage infiltration and cardiomyocyte degeneration, were seen. In these, macrophages were often found to express ICAM-1, transforming growth factor- $\beta$  and vascular endothelial growth factor; the former two were also expressed by cardiomyocytes.

These results confirm that DCM is associated with diffuse myocardial remodeling processes. The observed multifocal cell-rich lesions might result from reduced tissue perfusion. Macrophages and cardiomyocytes seem to actively contribute to these

processes, which ultimately lead to cardiac dilation and dysfunction. The precise role of the involved cells and the factors initiating the remodeling process still need to be identified.

**Keywords:** dilated cardiomyopathy, dogs, fibrosis, histology, immunohistology, inflammation, macrophages, morphometry



Dilated cardiomyopathy (DCM) is the most common cardiac disease in large breed dogs and is characterized by cardiac chamber dilation, systolic dysfunction and, in some cases, ventricular arrhythmia, which is eventually followed by congestive heart failure and/or sudden death.<sup>39,49,53,57</sup> The clinical diagnosis of DCM is based on echocardiographic findings, excluding other cardiac or systemic diseases and medications, such as treatment with anthracycline,<sup>35</sup> that may induce similar changes.<sup>11,39,49,53</sup>

Gross post mortem examination of the canine DCM heart reveals eccentric, primarily left ventricular hypertrophy and secondary left atrial dilation.<sup>11,53</sup> The histological changes, however, appear not to be very specific and are usually reported as mild: variation in myocyte size, myocyte degeneration and necrosis, and myocardial fibrosis of variable extent have been described.<sup>4,13,29,44,56</sup> According to the literature there are two distinct histological patterns which can predominate one over the other depending on the affected dog breed. The “fatty infiltration-degenerative” (FID) type, with myofiber degeneration, fibrosis and adipocyte infiltration, is mainly described in Boxers and Doberman Pinschers.<sup>54</sup> The “attenuated wavy fiber” (AWF) type, which is characterized by myofiber atrophy with a long wavy appearance of fibers, is seen in several large and medium-sized breeds, including Boxers and Doberman Pinschers.<sup>54</sup> More recent studies described further myocardial alterations, such as a change in the cardiomyocyte phenotype (reduced desmin expression) and an increase in vimentin-positive cells in the left atria, a mild mononuclear inflammatory infiltration in the interstitium of both atria and ventricles,<sup>28,29</sup> and hypertrophy of coronary vessel walls.<sup>30</sup>

Progress has also been made regarding the etiology of DCM, and genes associated with the disease are identified in Boxers, Doberman Pinschers and Irish Wolfhounds.<sup>40,41,45,49</sup>

Following numerous studies conducted on small and large experimental animal models of both cardiomyopathies and myocardial infarction,<sup>7,8,25</sup> it is generally accepted that most pathological processes affecting the myocardium, including DCM, result in a sequence of structural and functional changes known as myocardial remodeling.<sup>8,48</sup> Myocardial remodeling is in general prompted by cardiomyocyte injury, followed by an inflammatory reaction that is mediated by different cell types including neutrophils, macrophages and lymphocytes, and regulated by several factors, i.e. pro-inflammatory cytokines, adhesion molecules and extracellular matrix degrading enzymes (e.g. matrix metalloproteinases, MMPs).<sup>1,19,48</sup> Anti-inflammatory cytokines and growth factors such as transforming growth factor- $\beta$  (TGF- $\beta$ ) are subsequently involved in the reparative phase, promoting differentiation of fibroblasts into myofibroblasts, and extracellular matrix deposition.<sup>5,9,19,20</sup> However, this repair process can also result in excessive fibrosis.<sup>19</sup> Although sharing common pathways, depending on the type and extent of the initiating injury, different cellular and extracellular components are involved and the outcome may vary.<sup>3,48</sup>

Recent studies of our group confirmed increased myocardial transcription of inflammatory cytokines, MMPs and their inhibitors in dogs with cardiac diseases, suggesting a general activation of the inflammatory system in the myocardium in association with cardiac diseases.<sup>16,18</sup>

We hypothesize that the inflammatory and remodeling processes that are postulated to occur in the myocardium in association with canine DCM have consistent histopathological correlates in addition to those changes described so far. Therefore, the aim of the present study was to thoroughly assess the myocardium of dogs with clinically and grossly confirmed DCM for any pathological features and potential quantitative

changes, to gain further information on the pathomechanisms underlying DCM.

## **Materials and Methods**

### *Animals and Sample Collection*

The study was conducted on the hearts of 23 dogs: 17 dogs with DCM, and 6 dogs with diseases not involving the heart (control group) (Supplemental Tables S1 and S2). The dogs were all euthanized, except for dog 1.16, which suffered sudden death on a walk. Among the 17 dogs with DCM were ten Great Danes, six Doberman Pinschers and one Bullmastiff, they had a mean age of 6.4 years (range: 4 to 10 years). Nine dogs were female (4 of these were neutered) and 8 were male (of which 1 was neutered). The dogs in the control group represented various breeds and had a mean age of 7 years (range: 0.5 to 11 years); each three were male and female neutered.

At different time points prior to death, echocardiography had been carried out in all dogs with DCM to diagnose the disease, except for dog 1.16. For this dog, DCM was diagnosed on gross and histological cardiac findings during full necropsy. Further clinical investigations of the dogs with DCM had been performed on the discretion of the attending clinician (a board-certified cardiologist or a cardiology resident under direct supervision of a board-certified cardiologist), and included a complete blood count, biochemistry, electrocardiography and/or thoracic radiographs, depending on patient presentation. Dogs with non-cardiac diseases were euthanized on request of the owners due to grave prognoses (Supplemental Table S2). These dogs underwent investigations according to their presentation and based on the assessment of the attending clinician. Dogs underwent a partial (thoracic cavity) diagnostic post mortem examination with the

owners' consent. Hearts were removed and grossly examined for any pathological changes. Samples were collected from left atrium (LA) and right atrium (RA), left ventricular free wall (LV), right ventricular free wall (RV), and interventricular septum (IVS) for histological examination and, in selected cases (4 DCM and all control dogs) for RNA extraction (Supplemental Table S1 and S2). To obtain the samples, the lower half of the heart was separated by a cross section, and a sample from each of the mid LV, IVS, and RV towards the heart base was obtained. One cross-sectional slice of the removed apex was processed for histology after fixation, in addition to longitudinal sections of the LV, IVS, and RV. To ensure optimal complementarity, samples for RNA extraction were collected next to these areas.

#### *Histological, Immunohistological and Fluorescence Examinations*

Myocardial samples were fixed in 10% neutral-buffered formalin and routinely paraffin wax embedded. Consecutive sections (3 - 5 µm) were prepared and routinely stained with hematoxylin eosin and the van Gieson (VG) stain for the demonstration of collagen deposition. In 15 DCM cases (Supplemental Table S1) and all control hearts, additional sections were subjected to immunohistological and fluorescence staining.

The specimens were evaluated by light microscopy and assessed for any histopathological changes including those previously described in DCM, such as fatty infiltration, wavy fibers, fibrosis, and cardiomyocyte necrosis/degeneration.<sup>54</sup>

Immunohistology was performed using a Dako autostainer (Dako, Glostrup, Denmark) or the Discovery XT autostainer (Ventana Medical System, Inc., Tucson, USA). It served to detect leukocytes (CD18+, MHC II+), specifically, T cells (CD3+), B cells (CD20+) and macrophages (calprotectin+, Iba-1+), blood vessels, i.e. vascular endothelial cells

(Factor VIII+, CD31+) and smooth muscle cells ( $\alpha$ -smooth muscle actin ( $\alpha$ -SMA)+), and relevant mediators, i.e. TGF- $\beta$ 1, vascular endothelial growth factor (VEGF) and its receptor (Flk-1), and intercellular adhesion molecule 1 (ICAM-1). Antibodies with antigen retrieval and detection methods are listed in Supplemental Table S3. Briefly, after deparaffination, antigen retrieval was performed for all antigens except for  $\alpha$ -SMA and CD20, by incubation of the slides with citrate buffer (pH 6) at 98°C for 10 min, or with EDTA buffer (pH 9) at 98°C for 20 min. Endogenous peroxidase was blocked by incubation with hydrogen peroxide solution for 10 min. Sections were incubated with horse serum for 30 min at room temperature, followed by the primary antibodies and matching secondary antibodies; different detection kits were then applied. Sections were washed with phosphate buffered saline between each incubation step (pH 8). Finally, sections were counterstained with hematoxylin for 40 s and mounted.

Consecutive sections incubated with an isotype-matched irrelevant antibody or without the primary antibody served as negative controls. A chronic inflammatory process with granulation tissue formation served as positive control tissue.

The immunohistological staining was evaluated based on the morphology and location of the positive cells (vascular endothelial cells, smooth muscle cells in vessel wall, interstitial cells, lymphocytes and cardiomyocytes) as well as their distribution (scattered, multifocal or diffuse).

A further section underwent fluorescence staining to mark cell nuclei, using the ProLong Diamond Antifade Mountant with DAPI (4', 6-diamidino-2-phenylindole; Invitrogen). Briefly, after deparaffination and rehydration, sections were incubated with DAPI for 24 h at room temperature in the dark and then mounted.

### *Histomorphometric Analysis*

Sections from RV, LV and IVS from 15 dogs with DCM (Supplemental Table S1) and from all control dogs (Supplemental Table S2) stained with the VG stain, for  $\alpha$ -SMA, Iba-1 and with DAPI fluorescence and exhibiting consistent staining quality throughout the entire section were scanned (NanoZoomer-XR C12000; Hamamatsu, Japan) to obtain high resolution digital images. These were subsequently analyzed with the Visiopharm Integrator System (VIS, version 4.5.1.324, Visiopharm, Hørsholm, Denmark), considering the following parameters: overall cell number (based on the number of DAPI-positive nuclei), percentage area occupied by collagen fibers (based on the percentage of VG positive fibers), number of interstitial macrophages and blood vessels (based on the number of Iba-1- and  $\alpha$ -SMA-positive cells, respectively), and the respective proportion of tissue occupied by a) cardiomyocytes (interpreted as contractile tissue), b) collagen fibers, and c) fiber- and cell-free interstitial space (all assessed in the VG-stained section).

To specify, for each section, regions of interest with a size of 0.237 mm<sup>2</sup> (the area of a high power field with one ocular of 22 mm field of view) were randomly selected across the myocardium from areas free of focal cell-rich lesions. For DAPI,  $\alpha$ -SMA and Iba-1 and VG, positive cells and percentage of VG-positive fibers were counted in 20 regions of interest per section. In the VG-stained sections the areas comprised of a) cardiomyocytes, b) collagen fibers, and c) fiber- and cell-free interstitial space) were quantified within 10 regions of interest per section.

### *Relative Quantification of Cytokine and Remodeling Marker Transcription*

From selected DCM cases (1.10, 1.11, 1.14, and 1.15; Supplemental Table S1) and the

control dogs (which were partly used in previous studies<sup>16,17</sup>) myocardial samples could be collected within 1 h after death. These were stored in RNAlater (Thermo Fisher, Waltham, MA, USA) at -20°C until further use. Reverse transcriptase quantitative PCR (RT-qPCR) was carried out as previously described.<sup>15</sup> Published primer sequences were used for the canine housekeeping gene GAPDH, ICAM-1, cytokines (interleukin [IL]-1, -6, -8, -10, TNF- $\alpha$ , TGF- $\beta$ ), matrix metalloproteinase (MMP)-1, -2, -3, -9, -13, tissue inhibitor of MMP (TIMP)-1, -2, -3, -4, and lysyl oxidase.<sup>16,18,42</sup> The relative transcription levels of all markers were calculated using GAPDH and the  $2^{-\Delta Ct}$  method, as previously reported; all dogs have been part of previous studies the results of which have been published in different contexts.<sup>16,18</sup> From one dog with DCM (case 1.10) cardiomyocytes were collected using laser microdissection; RNA was extracted and qPCR was carried out as previously reported.<sup>16,18</sup>

### *Statistical Analyses*

Statistical analysis was carried out using SPSS. Distribution of data obtained from histomorphometry and qPCR was analyzed applying graphical Q-Q plots, Kolmogorov Smirnov and Shapiro-Wilk tests. Data were not normally distributed for  $\alpha$ -SMA, VG, ICAM-1, cytokines, MMP and TIMPs. Results from dogs with DCM and control dogs and results for different cardiac regions were therefore compared using Kruskal-Wallis and Mann Whitney U tests for not normal distributed data and 1-way ANOVA and unpaired t-tests for normal distributed data. Statistical significance was defined as  $P < 0.05$ .

## Results

### *Study Population*

With a mean age of 6.4 ( $\pm 1.6$ ) and 7 ( $\pm 3.6$ ) years, respectively, dogs with DCM and control dogs were of similar age ( $p=0.531$ ). Among the dogs with DCM, the 10 Great Danes had a mean age of 6 years ( $\pm 1.5$ ) and were overall slightly younger than the six Doberman Pinschers, which had a mean age of 7 years ( $\pm 1.8$ ). However, the age difference was not significant ( $p=0.247$ ).

### *Gross Findings*

Grossly, the hearts from dogs with DCM showed the previously reported macroscopic changes,<sup>11,53</sup> including cardiomegaly and chamber dilation (primarily of LA and LV). The hearts of control dogs were macroscopically unremarkable.

*The DCM myocardium exhibits diffuse widening of the interstitium with increase in collagen deposition and macrophages, and relative reduction of the contractile tissue.*

All hearts were first screened for the presence of those histological features of DCM that are known from the literature.<sup>11,38,54</sup> In 12 DCM cases (6/6 Doberman Pinschers, 5/10 Great Danes, the Bullmastiff), changes consistent with the FID type were detected, in the LV and/or IVS, and in half of the cases ( $n=6$ ; 4 Doberman Pinschers, 1 Great Dane and the Bullmastiff) also in the RA, RV or LA. Changes consistent with the AWF type, represented by multifocal areas with thin myofibers that showed a wavy appearance, were only detected in Great Danes (7/10), most frequently in the RA ( $n=5$ ), followed by the RV ( $n=3$ ), LV and IVS (each  $n=2$ ). The results are listed in Supplemental Table S1. Neither change was observed in the control hearts.



In 5/17 DCM dogs (4 Great Danes and 1 Doberman Pinscher; 1.1, 1.2, 1.6, 1.10, 1.12) vascular changes, represented by mild media hypertrophy of intramural arteries were observed;<sup>13,30</sup> a focal chronic mural thrombus was detected in the LA of one Great Dane (1.10).

In comparison to the myocardium of the control dogs, the interstitium of the DCM myocardium appeared overall wider and more cellular (Figs. 1, 2). In most cases, this finding was most prominent in the LV and IVS. The interstitial cells were generally round to spindle shaped, with a moderate to high amount of cytoplasm and oval to round nuclei. Some were more slender and resembled fibroblasts, but did not appear associated with collagen deposition (Fig. 3). Regardless of their shape, the majority of these cells were identified as macrophages, as they were found to express Iba-1, CD18 and MHC II (Fig. 4a-c). Interestingly, occasional intact cardiomyocytes distant from lesions exhibited strong cytoplasmic MHC II expression (data not shown). Calprotectin expression was observed in monocytes within vessel lumina and in occasional elongated interstitial cells, suggesting these had recently emigrated from the blood into the tissue.<sup>19</sup> A small proportion of the spindle shaped cells showed  $\alpha$ -SMA expression (Fig. 5a). Otherwise,  $\alpha$ -SMA positive cells were seen to surround small blood vessels, as confirmed by the matching arrangement of endothelial cells (FVIII-related antigen+; Fig. 5b); the latter were found to occasionally express Iba-1 and MHC II (Fig. 4a, c). Occasional individual T cells (CD3+) and B cells (CD20+) were also seen. Apart from the above-mentioned occasional “wavy fibers” and mild degenerative changes (rare loss of striation and scattered cytoplasmic vacuolization), the cardiomyocytes appeared unaltered.

A morphometric approach was taken to substantiate the above findings. Assessment of

the control dogs showed that the unaltered myocardium exhibits a similar overall cellularity (DAPI+ nuclei), proportion of contractile tissue, interstitial width (optically empty space plus collagen fibers) as well as a similar amount of small vessels ( $\alpha$ -SMA+ vascular structures) and macrophages (Iba-1+) in the interstitium in all examined cardiac regions (i.e. LV, RV, IVS; Table 1A).

In DCM, the myocardium exhibited an overall significantly lower cellularity (DAPI+ nuclei) than in control dogs. This was coupled with a significant increase in the number of Iba-1+ interstitial macrophages and a significantly lower relative proportion of contractile tissue, as well as an increased proportion of both fiber- and cell-free interstitial space and interstitial collagen (Table 1B).

A comparison of these parameters in the different cardiac regions (LV, RV, IVS) of dogs with DCM and control dogs confirmed these results. The proportion of fiber- and cell-free interstitial space was significantly increased and the proportion of contractile tissue significantly reduced in all three regions in DCM dogs (Table 1A). Similarly, DCM dogs also exhibited a decreased cellularity and an increase in interstitial collagen, but the difference was significant only in the LV and IVS. Interestingly, the amount of Iba-1+ interstitial macrophages was increased in both LV and IVS, but the difference was only significant in the LV (Table 1A). A comparison of the different cardiac regions in DCM showed also region-dependent differences for several parameters. The number of interstitial macrophages (Iba-1+) was significantly higher in the LV and IVS than in the RV. The interstitial collagen content was higher in the LV than in the IVS, whereas the proportion of contractile tissue (area covered by cardiomyocytes) was higher in the IVS than in the LV (Table 1A).

There was no significant difference in the number of interstitial vessels ( $\alpha$ -SMA+

structures) between both groups of dogs and in the different cardiac regions in both groups (Table 1).

*The DCM myocardium exhibits focal lesions, representing areas of fibroblast and macrophage accumulation and new vessel formation*

In 14 DCM cases, focal to multifocal, occasionally coalescing lesions, ranging between approximately 0.1 and 5 mm in diameter (Fig. 6a), were found in addition to the diffuse changes. These consisted of focal expansion of the interstitium and replacement of cardiomyocytes by cell-rich infiltrates containing differentiated vessels and abundant round to elongate cells with a morphology similar to the interstitial cells described above (Fig. 6b). A large proportion of these cells were identified as macrophages (Iba-1+, CD18+, MHC II+) (Fig. 7a-c). However, staining for  $\alpha$ -SMA revealed that the infiltrates also contained large amounts of small vessels (ranging in diameter between approximately 10 and 50  $\mu$ m; Fig. 7d) which was confirmed by staining for FVIII-related antigen and CD31, both highlighting the inner ring of endothelial cells and the presence of a small vascular lumen. The endothelial cells were occasionally found to also express Iba-1 (Fig. 7a) and MHC II (Fig. 7c). Vessels clearly dominated in some areas of the lesions (Fig. 8). Collagen fibers were found in small amounts between the cells within the lesions and replacing or surrounding individual degenerated cardiomyocytes. They were generally thin and loosely arranged, rarely forming more mature, dense fibrous tissue deposits (Fig. 9). Residual cardiomyocytes entrapped within the lesions displayed degenerative changes (swollen and vacuolated sarcoplasm) or necrosis. When present, focal lesions were seen in at least one of the five examined areas of the heart, most frequently in the LV (12/17), IVS (6/17) and RA (5/17) (Supplemental Table S1). In the

control dogs, the myocardium did not exhibit any of the above described histological changes.

*The pathological changes in the DCM myocardium are associated with significant upregulation of cytokines and remodeling markers*

As previously described, the normal canine myocardium exhibits constitutive expression of cytokines and remodeling markers.<sup>16,18</sup> In the present study we could show that this is also true for the adhesion molecule ICAM-1. In comparison, dogs with DCM showed significantly higher myocardial transcription of ICAM-1, TNF- $\alpha$ , IL-1, IL-8, IL-10, MMP-2, TIMP-1, and lysyl oxidase (Table 2). Laser microdissection with subsequent qPCR confirmed cardiomyocytes as a source of all markers tested with this approach, i.e. ICAM-1, TNF- $\alpha$ , IL-8, TGF- $\beta$ , MMP-2, TIMP-1 and TIMP-2. For ICAM-1 and TGF- $\beta$ , immunohistology was also applied and confirmed that morphologically unaltered cardiomyocytes produce both proteins, at low (ICAM-1) and very low (TGF- $\beta$ ) level in control hearts, and moderately (ICAM-1) and weakly (TGF- $\beta$ ) in DCM (Figs. 10-15). VEGF and its receptor, Flk1, were not expressed in the myocardium of control dogs, and VEGF expression was not detected in cardiomyocytes in DCM either (Figs. 16, 17). However, Flk1 was consistently expressed by cardiomyocytes in DCM (Figs. 18, 19). ICAM-1, TGF- $\beta$  and VEGF were also expressed in a proportion of cells within the focal lesions, mainly with the morphology of macrophages (Figs. 12, 15, 17). Interestingly, the mononuclear cells in the interstitium were often strongly TGF- $\beta$  positive (Fig. 14), but showed only weak ICAM-1 (Fig. 11) and neither VEGF nor Flk1 expression (Figs. 16, 18). Endothelial cells of both intralesional and extralesional vessels occasionally showed weak ICAM-1, TGF- $\beta$ , and Flk1 expression. A similar expression was seen occasionally

in vessels in the control hearts.

## **Discussion**

The present study represents a detailed investigation into the pathological changes in canine DCM, a disease associated with cardiac remodeling and of so far largely unknown pathogenesis.<sup>30,48,52</sup> Our results confirm a number of previously described histological changes as consistent features of canine DCM.<sup>54</sup> The so-called FID type was primarily found in Doberman Pinschers and the Bullmastiff.<sup>54</sup> These dogs did not show changes consistent with the AWF type. Great Danes on the other hand exhibited either FID or AWF changes, or both. Similar to previously published studies, these results suggest breed-dependent differences in the underlying pathogenesis or in the cardiomyocyte response to injury<sup>33,53,55</sup>, which might also be the cause of breed differences in clinical presentations.<sup>35,49,56</sup> Interestingly, FID changes were found to affect both the left and right heart, whereas AWF changes were more prominent in the right (RA and RV); this differs from a previous study undertaken in several dog breeds that reported wavy fibers as most abundant in the LV.<sup>54</sup>

Besides these known morphological features, the present study revealed more subtle diffuse myocardial changes in all DCM hearts, and, in addition, cell-rich focal lesions in a large proportion of cases, both without any relation to the presence of AWF or FID changes. To specify, the diffuse changes consisted of a relative reduction of the contractile tissue in association with an expansion of the interstitium due to an overall widening of the fiber- and cell-free space and an increase in the amount of interstitial collagen. Alongside this, an overall significantly reduced cellularity was observed despite

a significant increase in interstitial macrophages (Iba1+); this indicates that DCM is associated with loss of cardiomyocytes and thereby of contractile tissue.

Taken together these findings point towards individual cardiomyocyte injury and loss as the initial pathogenic process. This suggests that canine DCM differs from human primary DCM where the overall cell number does not change and an increase in cardiac muscle mass is observed as a result of compensatory cardiomyocyte hypertrophy.<sup>2</sup>

Further in depth studies would be required to confirm that canine DCM is indeed not associated with a change in cardiomyocyte size.

The focal cell-rich lesions were found more or less randomly distributed in most (14/17) DCM hearts where they were most prevalent and intense in the LV, followed by the IVS. Macrophages (Iba-1+, CD18+, MHC II+) were also abundant in these lesions. Both here and in the interstitium, they could result from local proliferation of resident cardiac macrophages and from monocyte recruitment.<sup>23,27</sup> Since calprotectin, a myeloid cell marker expressed by neutrophils, monocytes and recently blood derived, but not mature macrophages,<sup>19</sup> was found to be expressed only rarely in myocardial macrophages, it is likely that the vast majority were tissue-resident macrophages or resulted from local proliferation of macrophages recruited at an earlier stage.<sup>33</sup> Given the large heterogeneity of macrophage phenotypes and functions,<sup>11,18,21,21</sup> it is not clear if macrophages involved in the response to cardiac injury have a pro-inflammatory role and contribute to adverse cardiac remodeling, or have instead a reparative and cardioprotective function.<sup>12,20,27</sup> It has been postulated that resident macrophages are more likely to have a role in tissue repair processes in cardiac injury.<sup>12</sup> However, in the present study, immunohistology showed that macrophages in the focal lesions expressed TGF- $\beta$ , ICAM-1, VEGF, and, though less abundantly, its receptor, Flk1,

suggesting a dual function, i.e. both a reparative and an inflammatory role in canine DCM. In rats, ICAM-1, a cell adhesion molecule critical for leukocyte recruitment, mediates adhesion of macrophages to cardiomyocytes.<sup>6,45</sup> Such macrophage adherence can result in decreased cardiomyocyte contractility via the expression of TNF- $\alpha$ , oxygen free radicals and nitric oxide.<sup>45</sup> Laser microdissection with subsequent qPCR as well as immunohistology confirmed that cardiomyocytes produce ICAM-1, cytokines and remodeling enzymes. This suggests that both macrophages and cardiomyocytes might contribute to cardiomyocyte damage and/or dysfunction and the pathogenic process in dogs with DCM. ICAM-1 and cytokine upregulation also suggest an inflammatory state of the DCM myocardium. Inflammatory cytokines like TNF- $\alpha$  and IL-1, and chemokines regulate collagen turnover. These cytokines are involved in the dysregulation of MMP and TIMP expression<sup>8,10</sup> and inhibition of collagen degradation. This contributes to fibrosis, as observed in the dogs with DCM, and to decreased myocardial contractility and progression of heart failure, as reported for human DCM.<sup>32,47,48</sup> In particular, upregulation of MMP-2, TIMP-1 and TIMP-2 has been described in non-ischemic human DCM and in experimental conditions in dogs.<sup>36,37,46,52</sup> which is similar to the increase of MMP-2 and TIMP-1 found in the DCM dogs. Furthermore, TGF- $\beta$  that was expressed by cardiomyocytes as well as by lesional and interstitial macrophages might contribute to the increase in collagen observed in the DCM dogs. Cardiomyocytes under stress conditions or undergoing necrosis are known to be able to contribute to fibrosis through the production of TGF- $\beta$ .<sup>22</sup> TGF- $\beta$  exerts pro-fibrotic effects through the proliferation and differentiation of fibroblasts into myofibroblasts,<sup>5,9,10</sup> cells that were likely present both among the interstitial macrophage population and within the focal cell-rich lesions in the canine DCM myocardium.

In addition to the macrophage infiltration, the focal cell-rich lesions exhibited abundant small vessels indicative of neovascularization, whereas collagen deposition was limited. Individual degenerating/necrotic cardiomyocytes were found in the periphery of or entrapped within the lesions. The morphological evidence of neovascularization was associated with VEGF expression within infiltrating cells (most likely macrophages) in the lesions. These macrophages also produce TGF- $\beta$ ,<sup>26,55</sup> which, next to hypoxia, further stimulates VEGF production.<sup>26,51</sup>

Interestingly, the macrophages with higher pro-angiogenic potential have been shown to belong to the anti-inflammatory subset of macrophages and might therefore be involved in a repair attempt of the observed lesions.<sup>31</sup>

We found evidence of substantial expression of the VEGF receptor Flk-1 by cardiomyocytes in DCM, with particular intensity in cardiomyocytes entrapped in the lesions. When binding to Flk-1, VEGF exerts its angiogenetic properties; this interaction might have further contributed to the observed new vessel formation.<sup>51</sup> Morphologically, the focal lesions resemble chronic myocardial infarcts:<sup>14</sup> infarct healing is associated, particularly in the dog, with an intense angiogenic response.<sup>7</sup> Considering that we did not observe changes that would directly explain these lesions, and taking into account the described diffuse changes, it appears most likely that the focal lesions are a consequence of focal cardiomyocyte necrosis as a result of reduced tissue perfusion. The latter might be the result of the increased distance between blood vessels and cardiomyocytes due to interstitial edema (indicated by the overall widening of the interstitial space) and collagen deposition, or might also derive from the reduced oxygen tension characteristic of the microenvironment of a chronically inflamed tissue.<sup>50</sup>



In summary, canine DCM is associated with diffuse myocardial remodeling processes and focal lesions in the majority of dogs. Both macrophages and cardiomyocytes might actively contribute to the pathogenic process through the production of cytokines, adhesion molecules and remodeling enzymes, which eventually leads to cardiac dilation and impaired cardiac function.

Interestingly, we found similar changes, i.e. generalized diffuse remodeling and focal lesions, with cardiomyocyte degeneration, increased fibrosis, macrophages and neovascularization in cats with hypertrophic cardiomyopathy, a disease with a very different phenotype.<sup>34</sup> The resemblance of results suggests similar pathophysiological processes. Further investigations are required to explain how these processes result in diseases with different structural and functional presentations and which are the roles of macrophages and cardiomyocytes, which appear primarily involved in the pathogenesis of both canine DCM and feline hypertrophic cardiomyopathy.

## **Acknowledgements**

We are grateful to the technical staff in the Histology Laboratory, Institute of Veterinary Pathology, Vetsuisse Faculty, University of Zurich, for excellent technical support, and to Prof. Mark Oyama, School of Veterinary Medicine, University of Pennsylvania, for providing us with the mouse anti-canine ICAM antibody. Thanks are due to Dr Giovanni Pellegrini, Laboratory for Animal Model Pathology, Institute of Veterinary Pathology, Vetsuisse Faculty, University of Zurich, for his support towards the morphometric study. The RT-qPCR work was supported by a grant from the University of Liverpool and a NSERC discovery grant (RGPIN-2017-04399) from the government of Canada.

## References

1. Anker SD. Inflammatory mediators in chronic heart failure: an overview. *Heart*. 2004;90:464–470.
2. Beltrami CA, Finato N, Rocco M, et al. The cellular basis of dilated cardiomyopathy in humans. *J Mol Cell Cardiol*. 1995;27:291–305.
3. Cohn JN, Ferrari R, Sharpe N. Cardiac remodeling-concepts and clinical implications: A consensus paper from an International Forum on Cardiac Remodeling. *J Am Coll Cardiol*. 2000;35:569–582.
4. Dambach DM, Lannon A, Sleeper MM, Buchanan J. Familial dilated cardiomyopathy of young Portuguese water dogs. *J Vet Intern Med*. 1999;13:65–71.
5. Darby IA, Laverdet B, Bonté F, Desmoulière A. Fibroblasts and myofibroblasts in wound healing. *Clin Cosmet Investig Dermatol*. 2014;7:301–311.
6. Davani EY, Dorscheid DR, Lee CH, van Breemen C, Walley KR. Novel regulatory mechanism of cardiomyocyte contractility involving ICAM-1 and the cytoskeleton. *Am J Physiol Heart Circ Physiol*. 2004;287:H1013-22.
7. Dewald O, Ren G, Duerr GD, et al. Of mice and dogs: species-specific differences in the inflammatory response following myocardial infarction. *Am J Pathol*. 2004;164:665–677.
8. Dixon JA, Spinale FG. Myocardial remodeling: cellular and extracellular events and targets. *Annu Rev Physiol*. 2011;73:47–68.
9. Dobaczewski M, Chen W, Frangogiannis NG. Transforming growth factor (TGF)- $\beta$

- signaling in cardiac remodeling. *J Mol Cell Cardiol.* 2011;51:600–606.
10. Dobaczewski M, Gonzalez-Quesada C, Frangogiannis NG. The extracellular matrix as a modulator of the inflammatory and reparative response following myocardial infarction. *J Mol Cell Cardiol.* 2010;48:504–511.
  11. Dukes-McEwan J, Borgarelli M, Tidholm A, Vollmar AC, Häggström J. Proposed Guidelines for the Diagnosis of Canine Idiopathic Dilated Cardiomyopathy. *J Vet Cardiol.* 2003;5:7–19.
  12. Epelman S, Lavine KJ, Beaudin AE, et al. Embryonic and adult-derived resident cardiac macrophages are maintained through distinct mechanisms at steady state and during inflammation. *Immunity.* 2014;40:91–104.
  13. Everett RM, McGann J, Wimberly HC, Althoff J. Dilated cardiomyopathy of Doberman pinschers: retrospective histomorphologic evaluation of heart from 32 cases. *Vet Pathol.* 1999;36:221–227.
  14. Falk T, Jönsson L. Ischaemic heart disease in the dog: a review of 65 cases. *J Small Anim Pract.* 2000;41:97–103.
  15. Fonfara S, Tew SR, Cripps P, Dukes-McEwan J, Clegg PD. Increased blood mRNA expression of inflammatory and anti-fibrotic markers in dogs with congestive heart failure. *Res Vet Sci.* 2012;93:879–885.
  16. Fonfara S, Hetzel U, Tew SR, Cripps P, Dukes-McEwan J, Clegg PD. Expression of matrix metalloproteinases, their inhibitors, and lysyl oxidase in myocardial samples from dogs with end-stage systemic and cardiac diseases. *Am J Vet Res.* 2013;74:216–223.
  17. Fonfara S, Hetzel U, Tew SR, Cripps P, Dukes-McEwan J, Clegg PD. Myocardial cytokine expression in dogs with systemic and naturally occurring cardiac

- diseases. *Am J Vet Res.* 2013;74:408–416.
18. Fonfara S, Hetzel U, Tew SR, Cripps P, Dukes-McEwan J, Clegg PD. Myocardial cytokine expression in dogs with systemic and naturally occurring cardiac diseases. *Am J Vet Res.* 2013;74:5–7.
  19. Frangogiannis NG. Regulation of the inflammatory response in cardiac repair. *Circ Res.* 2012;110:159–173.
  20. Frangogiannis NG. Inflammation in cardiac injury, repair and regeneration. *Curr Opin Cardiol.* 2015;2:240–245.
  21. Frangogiannis NG. Emerging roles for macrophages in cardiac injury: Cytoprotection, repair, and regeneration. *J Clin Invest.* 2015;125:2927–2930.
  22. Frangogiannis NG. Fibroblasts and the extracellular matrix in right ventricular disease. *Cardiovasc Res.* 2017;1453–1464.
  23. Frantz S, Nahrendorf M. Cardiac macrophages and their role in ischemic heart disease. *Cardiovasc Res.* 2014;102:1–9.
  24. Fujiu K, Wang J, Nagai R. Cardioprotective function of cardiac macrophages. *Cardiovasc Res.* 2014;102:232–239.
  25. Hanna N, Cardin S, Leung TK, Nattel S. Differences in atrial versus ventricular remodeling in dogs with ventricular tachypacing-induced congestive heart failure. *Cardiovasc Res.* 2004;63:236–244.
  26. Harmey JH, Dimitriadis E, Kay E, Redmond HP, Bouchier-Hayes D. Regulation of macrophage production of vascular endothelial growth factor (VEGF) by hypoxia and transforming growth factor beta-1. *Ann Surg Oncol.* 1998;5:271–278.
  27. Hulsmans M, Sam F, Nahrendorf M. Monocyte and macrophage contributions to cardiac remodeling. *J Mol Cell Cardiol.* 2016;93:149–155.

28. Janus I, Kandefer-Gola M, Ciaputa R, et al. The immunohistochemical evaluation of selected markers in the left atrium of dogs with end-stage dilated cardiomyopathy and myxomatous mitral valve disease - a preliminary study. *Ir Vet J.* 2016;69:18.
29. Janus I, Noszczyk-Nowak A, Nowak M, Ciaputa R, Kandefer-Gola M, Paśławska U. A comparison of the histopathologic pattern of the left atrium in canine dilated cardiomyopathy and chronic mitral valve disease. *BMC Vet Res.* 2016;12:3.
30. Janus I, Nowak M, Madej JA. Pathomorphological changes of the myocardium in canine dilated cardiomyopathy (DCM). *Bull Vet Inst Pulawy.* 2015;59:135–142.
31. Jetten N, Verbruggen S, Gijbels MJ, Post MJ, De Winther MPJ, Donners MMPC. Anti-inflammatory M2, but not pro-inflammatory M1 macrophages promote angiogenesis in vivo. *Angiogenesis.* 2014;17:109–118.
32. Kim HE, Dalal SS, Young E, Legato MJ, Weisfeldt ML, D'Armiento J. Disruption of the myocardial extracellular matrix leads to cardiac dysfunction. *J Clin Invest.* 2000;106:857–866.
33. Kipar A, Baumgärtner W, Kremmer E, Frese K, Weiss E. Expression of major histocompatibility complex class II antigen in neoplastic cells of canine cutaneous histiocytoma. *Vet Immunol Immunopathol.* 1998;62:1–13.
34. Kitz S, Fonfara S, Hahn S, Hetzel U, Kipar A. Feline Hypertrophic Cardiomyopathy, the Consequence of Cardiomyocyte-Initiated and Macrophage-Driven Remodeling Processes? *Vet Pathol (in Press).*
35. Lee YR, Kang MH, Park HM. Anthracycline-induced cardiomyopathy in a dog treated with epirubicin. *Can Vet J.* 2015;56:571–574.
36. Li YY, McTiernan CF, Feldman AM. Interplay of matrix metalloproteinases, tissue

inhibitors of metalloproteinases and their regulators in cardiac matrix remodeling. *Cardiovasc Res.* 2000;46:214–224.

37. Lin JM, Lai LP, Lin CS, Chou NK, Chiu CY, Lin JL. Left Ventricular Extracellular Matrix Remodeling in Dogs with Right Ventricular Apical Pacing. *J Cardiovasc Electrophysiol.* 2010;21:1142–1149.
38. Lobo L, Carvalheira J, Canada N, Bussadori C, Gomes JL, Faustino AMR. Histologic Characterization of Dilated Cardiomyopathy in Estrela Mountain Dogs. *Vet Pathol.* 2010;47:637–642.
39. Martin MWS, Stafford Johnson MJ, Celona B. Canine dilated cardiomyopathy: A retrospective study of signalment, presentation and clinical findings in 369 cases. *J Small Anim Pract.* 2009;50:23–29.
40. Meurs KM, Stern JA, Sisson DD, et al. Association of dilated cardiomyopathy with the striatin mutation genotype in boxer dogs. *J Vet Intern Med.* 2013;27:1437–1440.
41. Meurs KM, Fox PR, Norgard M, et al. A prospective genetic evaluation of familial dilated cardiomyopathy in the Doberman pinscher. *J Vet Intern Med.* 2007;21:1016–1020.
42. Oyama MA, Chittur SV. Genomic expression patterns of mitral valve tissues from dogs with degenerative mitral valve disease. *Am J Vet Res.* 2006;67:1307–1318.
43. Philipp U, Vollmar A, Häggström J, Thomas A, Distl O. Multiple loci are associated with dilated cardiomyopathy in irish wolfhounds. *PLoS One.* 2012;7:1–6.
44. Sandusky GE, Capen CC, Kerr KM. Histological and ultrastructural evaluation of cardiac lesions in idiopathic cardiomyopathy in dogs. *Can J Comp Med.* 1984;48:81–86.

45. Simms MG, Walley KR. Activated macrophages decrease rat cardiac myocyte contractility: importance of ICAM-1-dependent adhesion. *Am J Physiol*. 1999;277:H253-60.
46. Simpson S, Edwards J, Ferguson-Mignan TF, Cobb M, Mongan NP, Rutland CS. Genetics of human and canine dilated cardiomyopathy. *Int J Genomics*. 2015.
47. Spinale FG. Matrix metalloproteinases: Regulation and dysregulation in the failing heart. *Circ Res*. 2002;90:520–530.
48. Spinale FG. Myocardial Matrix Remodeling and the Matrix Metalloproteinases: Influence on Cardiac Form and Function. *Physiol Rev*. 2007;87:1285–1342.
49. Stephenson HM, Fonfara S, López-Alvarez J, Cripps P, Dukes-McEwan J. Screening for Dilated Cardiomyopathy in Great Danes in the United Kingdom. *J Vet Intern Med*. 2012;26:1140–1147.
50. Szade A, Grochot-Przeczek A, Florczyk U, Jozkowicz A, Dulak J. Cellular and molecular mechanisms of inflammation-induced angiogenesis. *IUBMB Life*. 2015;67:145–159.
51. Taimeh Z, Loughran J, Birks EJ, Bolli R. Vascular endothelial growth factor in heart failure. *Nat Rev Cardiol*. 2013;10:519–530.
52. Thomas CV., Coker ML, Zellner JL, Handy JR, Crumbley AJ, Spinale FG. Increased Matrix Metalloproteinase Activity and Selective Upregulation in LV Myocardium From Patients With End-Stage Dilated Cardiomyopathy. *Circulation*. 1998;97:1708–1715.
53. Tidholm A, Häggström J, Borgarelli M, Tarducci A. Canine Idiopathic Dilated Cardiomyopathy. Part I: Aetiology, Clinical Characteristics, Epidemiology and Pathology. *Vet J*. 2001;162:92–107.

54. Tidholm A, Jönsson L. Histologic Characterization of Canine Dilated Cardiomyopathy. *Vet Pathol.* 2005;42:1–8.
55. Uchida N, Nagai K, Sakurada Y, Shiota K. Distribution of VEGF and flt-1 in the normal dog tissues. *J Vet Med Sci.* 2008;70:1273–1276.
56. Vollmar AC, Aupperle H. Cardiac pathology in Irish wolfhounds with heart disease. *J Vet Cardiol.* 2016;18:57–70.
57. Wess G, Schulze A, Butz V, et al. Prevalence of dilated cardiomyopathy in Doberman Pinschers in various age groups. *J Vet Intern Med.* 2010;1–6.



## Figure Legends

**Figure 1.** Control heart, dog 2.3. Unaltered myocardium with tightly aligned cardiomyocytes. HE stain. **Figures 2-5.** DCM, heart, dog 1.15. **Figure 2.** The myocardium exhibits a widened interstitium with an increased amount of cells (arrow). HE stain. **Figure 3.** The interstitial cells (arrow) are round to spindle shaped, with an oval to round nucleus, sometimes more slender, resembling fibroblasts. HE stain. **Figure 4.** The majority of interstitial cells are macrophages, as they express Iba-1 (**a**), CD18 (**b**) and MHC II (**c**). Occasional endothelial cells in interstitial vessels are found to express Iba-1 (**a**) and/or MHC II (**c**). Immunohistology, hematoxylin counterstain. **Figure 5.** The interstitium exhibits abundant small vessels, identified on the outer layer of  $\alpha$ -SMA positive cells (smooth muscle cells, arrows) (**a**) and the (inner), FVIII-related antigen positive endothelial cell layer (**b**). A small proportion of the spindle shaped cells in the interstitium also showed  $\alpha$ -SMA expression (myofibroblasts; arrowheads) (**a**). Immunohistology, hematoxylin counterstain.

**Figures 6-9.** DCM, heart, dog 1.15. Focal lesions. **Figure 6.** Focal replacement of cardiomyocytes by a cell-rich infiltrate (**a**; M: myocardium with unaltered cardiomyocytes. **b**. The infiltrate contains differentiated vessels (arrows) and abundant round to elongate cells with a morphology similar to the interstitial cells observed in increased numbers throughout the entire myocardium. HE stains. **Figure 7.** A large proportion of cells in the infiltrate are identified as macrophages, based on the expression of Iba-1 (**a**), CD18 (**b**) and MHC II (**c**), intermingled with and partly outnumbering the  $\alpha$ -SMA positive cells that in the majority form small vessels (**d**). Occasional endothelial cells found to also express Iba-1 (**a**; arrowhead) and MHC II (**c**; arrowhead). Immunohistology, hematoxylin

counterstain. **Figure 8.** Vessels clearly dominated in some areas of the lesions.

Immunohistology, for the demonstration of  $\alpha$ -SMA, hematoxylin counterstain. **Figure 9.**

Small amounts of predominantly thin and loosely arranged collagen (arrowheads) between the cells within the lesions. Van Gieson stain. **Figures 10-12.** Expression of ICAM-1 in the myocardium. Immunohistology, hematoxylin counterstain. **Figure 10.**

Control heart, dog 2.2. Cardiomyocytes show weak ICAM-1 expression. **Figures 11 and 12.** DCM, heart, dog 1.15. **a.** Cardiomyocytes show moderate ICAM-1 expression. The interstitial cells exhibit only very weak staining (arrowheads). **b.** A substantial proportion of the mononuclear cells in the focal lesion exhibit ICAM-1 expression (arrowheads). Arrows: cardiomyocytes. **Figures 13-15.** Expression of TGF- $\beta$  in the myocardium. Immunohistology, hematoxylin counterstain. **Figure 13.** Control heart, dog 2.1. Cardiomyocytes show no or very weak TGF- $\beta$  expression. **Figures 14 and 15.** DCM, heart, dog 1.15. **a.** Cardiomyocytes exhibit very weak to weak TGF- $\beta$  expression, whereas the interstitial cells are often strongly TGF- $\beta$  positive (arrowheads). **b.** A substantial proportion of the mononuclear cells in the focal lesion exhibit ICAM expression (inset: arrowheads). Arrows: cardiomyocytes. **Figures 16 and 17.** DCM, heart, dog 1.15. Expression of VEGF in the myocardium. Immunohistology, hematoxylin counterstain. **Figure 16.** Cardiomyocytes as well as the interstitial cells (arrowheads) are VEGF-negative. **Figure 17.** A substantial proportion of the mononuclear cells in the focal lesion exhibit VEGF expression (inset: arrowheads). **Figures 18 and 19.** DCM, heart, dog 1.15. Expression of the VEGF receptor Flk1 in the myocardium. Immunohistology, hematoxylin counterstain. **Figure 18.** Cardiomyocytes exhibit moderate Flk1 expression, whereas the interstitial cells are Flk1 negative (arrowhead). **Figure 19.** The cells in the focal lesion are also Flk1 negative.

**Table 1.** Comparison of overall cellularity, number of interstitial small vessels, and macrophages, and percentage of area covered by cardiomyocytes, collagen and fibre- and cell-free interstitial space in the myocardium (right and left ventricle and interventricular septum) of control dogs and dogs with DCM.

**A.** Comparison of the different cardiac regions<sup>A</sup>.

	Control			DCM		
Parameters	RV	IVS	LV	RV	IVS	LV
	(n=5)	(n=5)	(n=6)	(n=5)	(n=8)	(n=11)
DAPI	1005	1014 <sup>1</sup>	988 <sup>2</sup>	744	760 <sup>1</sup>	768 <sup>2</sup>
	(±319)	(±237)	(±298)	(±80.0)	(±147.8)	(±127.8)
α-SMA	791	926	901	706	735	724
	(310-1066)	(411-972)	(553-947)	(512-1167)	(459-1125)	(434-1214)
Collagen	1.53	1.05 <sup>1</sup>	0.95 <sup>2</sup>	1.91	2.29 <sup>1,3</sup>	4.51 <sup>2,3</sup>
	(1.06-2.03)	(0.15-1.61)	(0.18-1.87)	(1.02-8.46)	(1.12-6.62)	(1.54-12.37)
Iba-1	59.8	53.8	46.6 <sup>1</sup>	37.2 <sup>2, 3</sup>	81.9 <sup>2</sup>	83.0 <sup>1, 3</sup>
	(±29.8)	(±26.9)	(±11.7)	(±23.9)	(±35.1)	(±27.1)
Cardiomyo-	86.8 <sup>1</sup>	90.5 <sup>2</sup>	89.3 <sup>3</sup>	66.3 <sup>1</sup>	73.6 <sup>2, 4</sup>	63.2 <sup>3, 4</sup>

cytes	(±4.4)	(±3.3)	(±6.1)	(±12.4)	(±10.4)	(±7.2)
Interstitial	11.7 <sup>1</sup>	8.8 <sup>2</sup>	9.7 <sup>3</sup>	30.6 <sup>1</sup>	24.9 <sup>2</sup>	31.8 <sup>3</sup>
space	(±4.0)	(±3.4)	(±5.7)	(±10.5)	(±10.2)	(±6.6)

<sup>A</sup>Results in each row that are significantly different from each other are marked by the same superscript number. Normal distributed results are reported as mean and standard deviation, not normal distributed data are reported as median and interquartile range.

DAPI, number of cells per 20 regions of interest (ROI), based on the number of DAPI positive fluorescent nuclei;  $\alpha$ -SMA, number of vessels per 20 ROIs, based on the number of  $\alpha$ -SMA positive vascular structures; Collagen, percentage area occupied by VG positive fibers in 20 ROIs; Iba-1, number of macrophages per 20 ROIs, based on the number of Iba-1 positive interstitial cells; Cardiomyocytes, percentage area occupied by cardiomyocytes in 10 ROIs in VG-stained section; Interstitial space, percentage area of fiber- and cell-free interstitial space in 10 ROIs in VG-stained section.

**B. Overall assessment, based on the available data for all three cardiac regions.<sup>B</sup>**

Parameters	Control (n=14)	DCM (n=23)	P-value
DAPI	1002 (±268)	761 ↓ (±124)	<b>0.003</b>
α-SMA	920 (310-1066)	724 (434-1214)	0.72
Collagen	1.17 (0.15-2.03)	3.08 ↑ (1.02-12.37)	<b>&lt;0.001</b>
Iba-1	53.4 (±23.1)	73.1 ↑ (±33.9)	<b>0.038</b>
Cardiomyocytes	88.9 (±4.8)	67.3 ↓ (±10.2)	<b>&lt;0.001</b>
Interstitial space	10.0 (±4.4)	29.2 ↑ (±8.9)	<b>&lt;0.001</b>

<sup>B</sup>Normal distributed results are reported as mean and standard deviation, not normal distributed data are reported as median and interquartile range.

Abbreviations:  $\alpha$ -SMA,  $\alpha$ -smooth muscle actin; DAPI, 4', 6-diamidino-2-phenylindole; DCM, dilated cardiomyopathy; Iba-1, ionized calcium binding adaptor molecule-1; IVS, interventricular septum; LV, left ventricle; RV, right ventricle.

**Table 2.** Relative ICAM-1, cytokine and remodeling marker mRNA expression in the myocardium of control dogs and dogs with DCM (relative expression using the Ct value of the respective marker to the Ct value of GAPDH was applied,  $2^{-\Delta Ct}$ ). Results are reported as median and interquartile range.

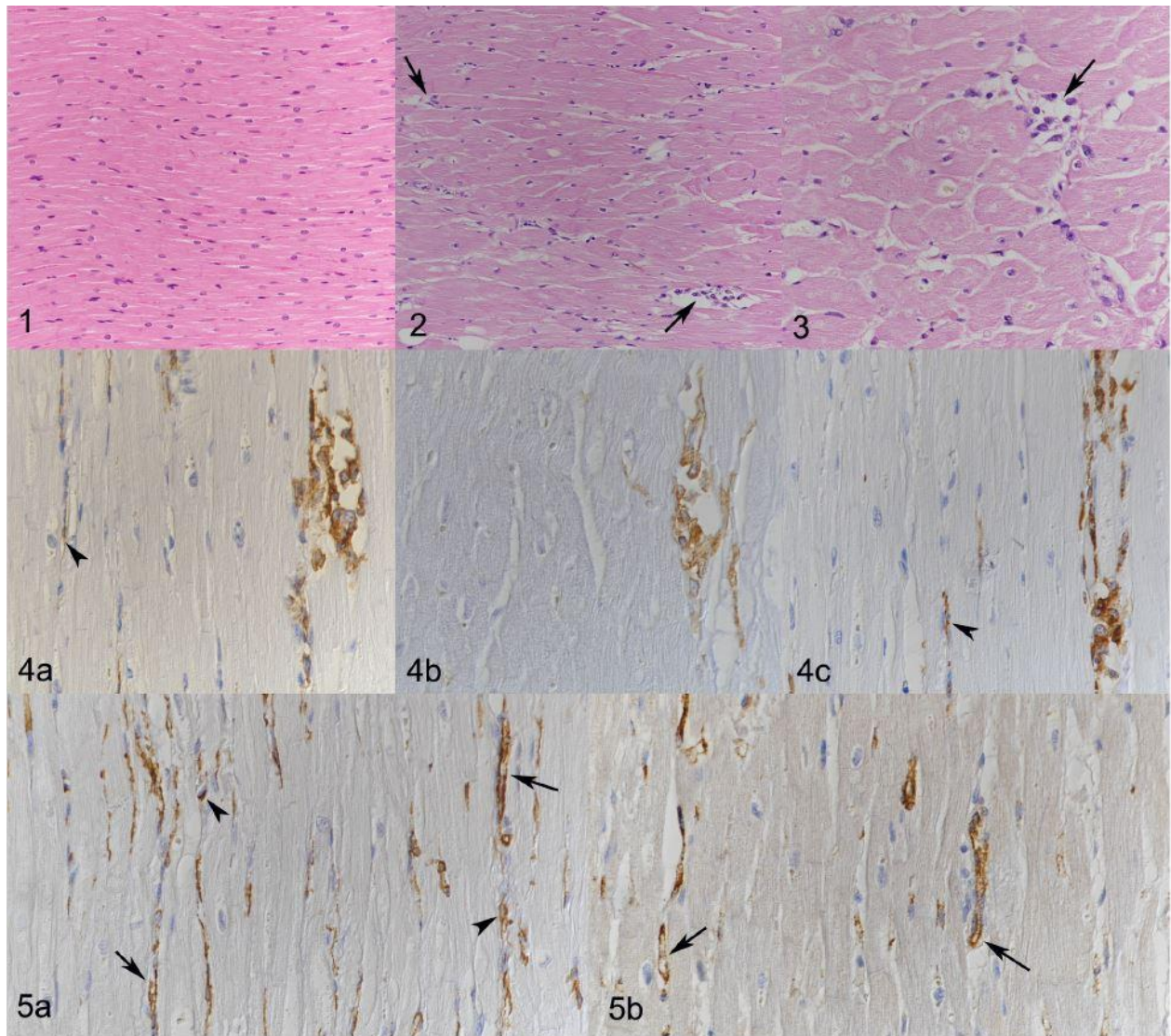
<b>Marker</b>	<b>Control (n=30<sup>a</sup>)</b>	<b>DCM (n=20<sup>a</sup>)</b>	<b>P-value</b>
ICAM	298 (107-761)	1277 ↑ (255-3934)	<b>0.003</b>
IL-1	7.6 (4.5-23.8)	19.4 ↑ (11.7-32.3)	<b>0.012</b>
IL-6	10.02 (3.23-24.2)	71.3 (6.97-144)	0.075
IL-8	47.2 (26.1-119.4)	232 ↑ (71.6-811)	<b>0.001</b>
IL-10	19.5 (12.8-38.3)	48.7 ↑ (32.1-153)	<b>&lt;0.001</b>
TNF- $\alpha$	4.14 (2.75-6.83)	12.4 ↑ (3.05-19.6)	<b>0.019</b>
TGF- $\beta$	3457 (1977-4960)	3555 (2622-4780)	0.406
MMP-1	1.97 (0.3-10.9)	2.49 (0.2-21.2)	0.621
MMP-2	230	980 ↑	<b>&lt;0.001</b>

	(52.4-386.2)	(318.6-2033.4)	
MMP-3	0.11	0.12	0.338
	(0.0-1.7)	(0.0-0.53)	
MMP-9	9.1	3.4	0.890
	(1.5-28.6)	(1.6-61.6)	
MMP-13	0.64	.37	0.053
	(0.18-1.41)	(0.75-3.88)	
TIMP-1	401	1173 ↑	<b>0.002</b>
	(229-1212)	(513-7563)	
TIMP-2	6801	10510	0.055
	(4783-9615)	(5516-18408)	
TIMP-3	18655	11735	0.075
	(6910-27788)	(5071-20188)	
TIMP-4	1777	3347	0.175
	(1325-3478)	(1609-4878)	
Lysyl	889	1795 ↑	<b>0.009</b>
oxidase	(403-1805)	(1078-3252)	

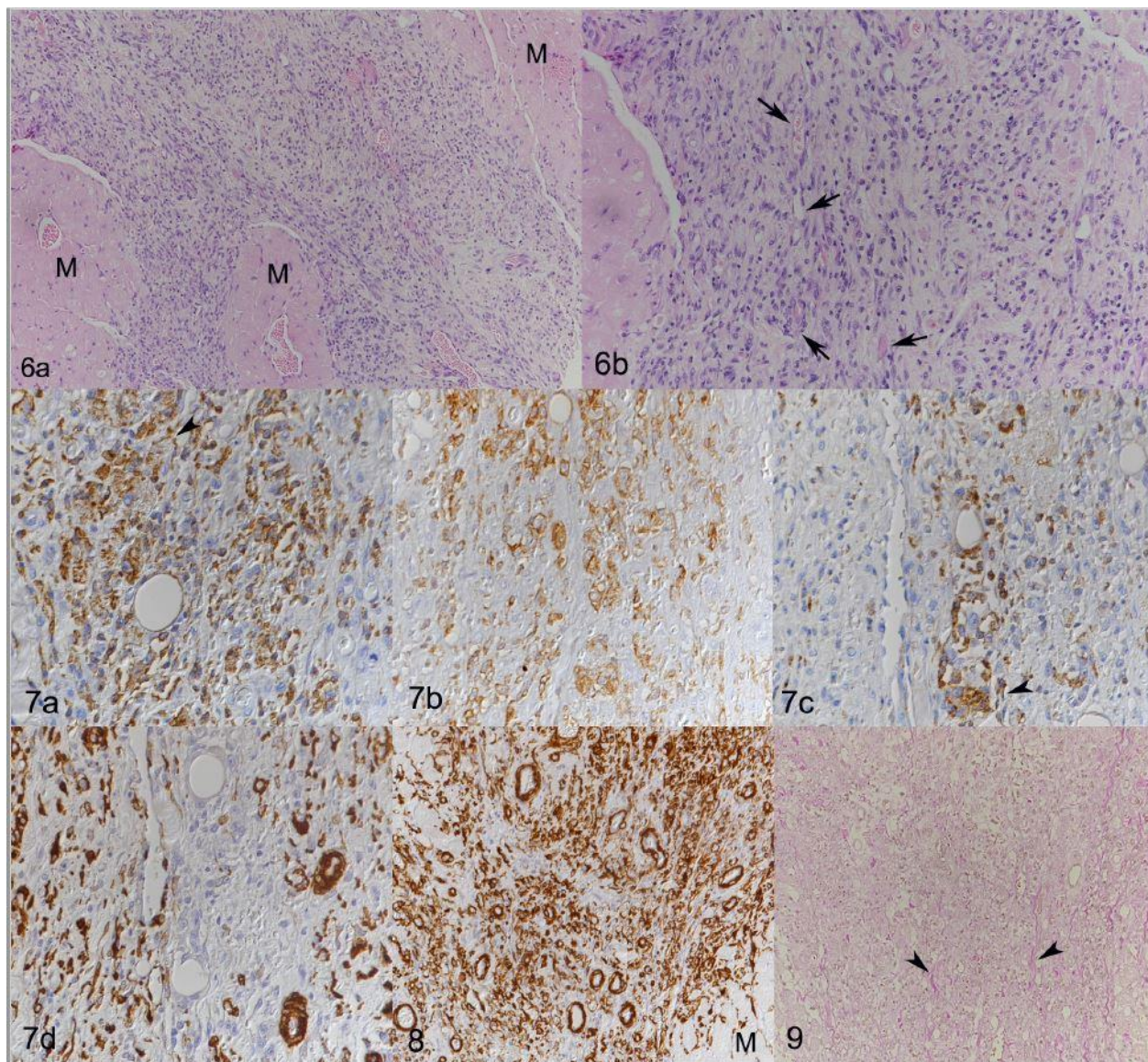
a: represents the total number of samples (LA, RA, LV, IVS and RV) examined for this group. P-values indicating significant differences are in bold.

Abbreviations: DCM, dilated cardiomyopathy; ICAM, intercellular adhesion molecule 1; IL, interleukin; MMP, matrix metalloproteinase; TGF, transforming growth factor; TIMP, tissue inhibitor of metalloproteinases; TNF, tumor necrosis factor.

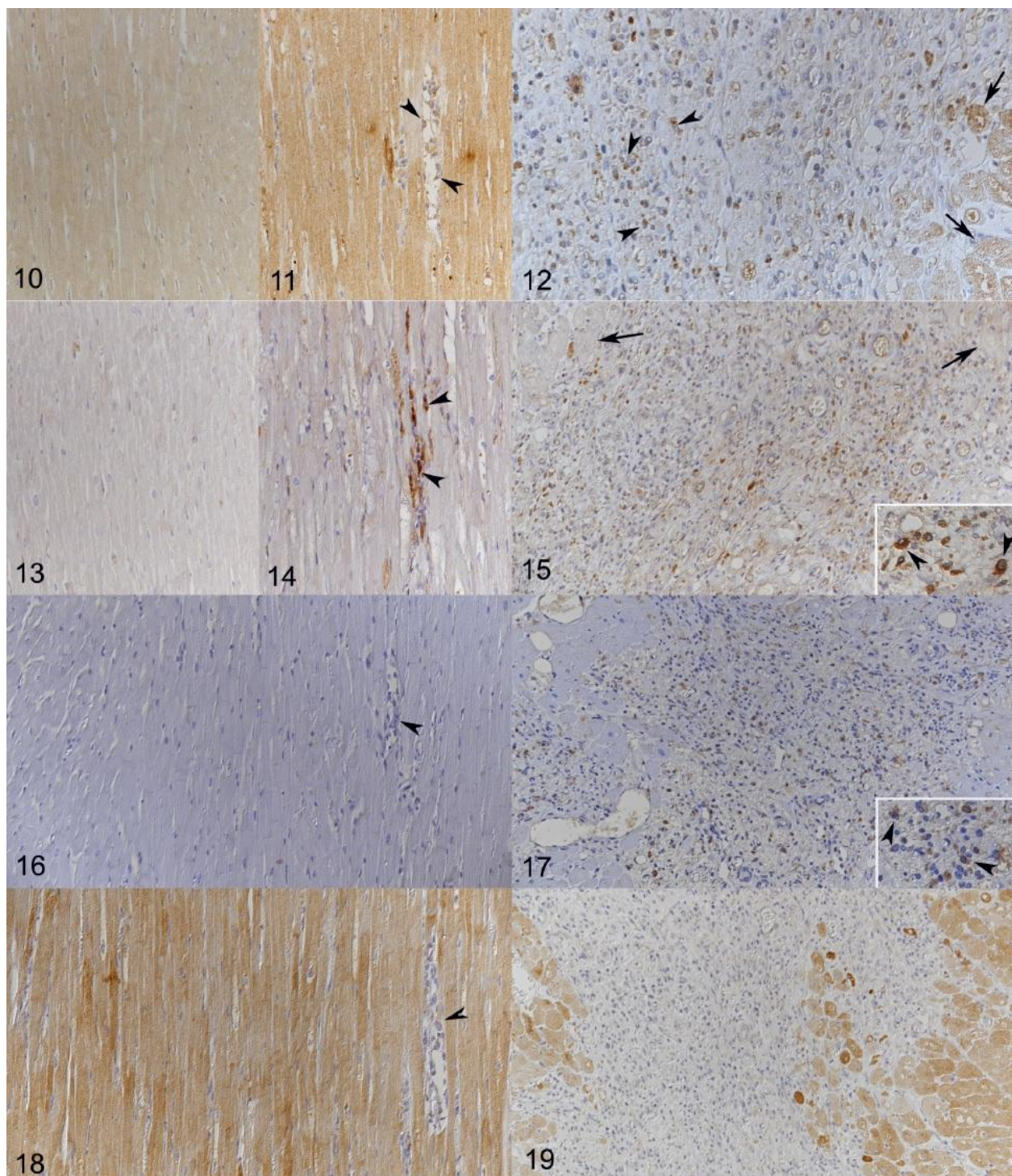












**Supplemental Table S1.** Dogs diagnosed with DCM. Breed, age and sex, presence and distribution of histological changes (fatty infiltration-degenerative type (FID), attenuated wavy fiber type (AWF), focal lesions), and examinations performed in addition to the histological evaluation and the immunohistological staining for  $\alpha$ -SMA and Iba-1.

Case No	Signalment			Histopathological changes in the myocardium			Further examinations
	Breed	Age (y)	Sex	FID	AWF	Focal lesions	
1.1	Great Dane	6	MN	nd	RA, RV	RA, LV	IH <sup>A</sup> , morphometry <sup>B</sup>
1.2	Great Dane	7	M	nd	LV, IVS	RA, LV	np
1.3	Great Dane	6	F	nd	RA, RV	nd	IH, morphometry
1.4	Great Dane	9	FN	nd	RA, RV, LA	LV, IVS	IH, morphometry
1.5	Great Dane	6	F	nd	LV, IVS	LV	IH, morphometry
1.6	Great Dane	4	FN	LV	RA	LV, IVS	IH, morphometry
1.7	Great Dane	5	M	IVS	RA	IVS	IH, morphometry
1.8	Great Dane	4	M	LV	nd	LV	IH, morphometry
1.9	Great Dane	7	F	LV	nd	RA	np
1.10	Great Dane	6	M	RV, LV, IVS	nd	RV, LA, LV, IVS	IH, morphometry, qPCR <sup>C</sup>

1.11	Bullmastiff	7	M	RV, LA, LV, IVS	nd	nd	IH, morphometry, qPCR
1.12	Doberman	6	FN	LV	nd	LV	IH, morphometry
1.13	Doberman	6	M	RA, RV, LA, LV	nd	LV	IH, morphometry
1.14	Doberman	10	FN	RA, RV, LA, LV, IVS	nd	nd	IH, morphometry, qPCR
1.15	Doberman	8	M	LV, IVS	nd	LV	IH, morphometry, qPCR
1.16	Doberman	7	F	RA, LV, IVS	nd	LV, IVS	IH, morphometry
1.17	Doberman	5	FN	RA, RV, LA, LV, IVS	nd	RA, LV, S	IH, morphometry

<sup>A</sup>IH: implies staining for one or more of the antigens listed in Supplemental Table S3, in addition to staining for  $\alpha$ -SMA and Iba-1.

<sup>B</sup>Morphometry: implies the morphometric assessment of van Giesson stained sections, sections stained by immunohistology for  $\alpha$ -SMA and Iba-1, and sections stained with DAPI fluorescence.

<sup>C</sup>qPCR: implies quantitative reverse transcriptase PCR for the cytokines and remodeling enzymes listed in Table 2.

Abbreviations: F, female; IVS, interventricular septum; LA, left atrium; LV, left ventricle; M, male; N, neutered; nd, not detected, np not performed, qPCR, quantitative reverse transcriptase PCR; RA, right atrium; RV, right ventricle; y, years.

**Supplemental Table S2.** Control animals, i.e. dogs that had suffered from diseases not involving the heart. Breed, age and sex, and examinations performed in addition to the histological evaluation and the immunohistological staining for  $\alpha$ -SMA and Iba-1.

Case No	Breed	Age (y)	Sex	Disease	Further examinations
2.1.	Labrador Retriever	0.5	M	Spinal fracture due to road traffic accident	IH <sup>A</sup> , morphometry <sup>B</sup> , qPCR <sup>D</sup>
2.2	German Shepherd	9	M	Hemangiosarcoma (spleen, liver)	IH, morphometry, qPCR
2.3	Cocker Spaniel	8	FN	Brain tumor	IH, morphometry, qPCR
2.4	Boxer	7	M	Brain tumor	IH, morphometry, qPCR
2.5	Cross breed	7	FN	Multicentric lymphoma	Morphometry, qPCR
2.6	Cross breed	11	FN	Pancreatic carcinoma	Morphometry, qPCR

---

<sup>A</sup>IH: implies staining for one or more of the antigens listed in Supplemental Table S3, in addition to staining for  $\alpha$ -SMA and Iba-1.

<sup>B</sup>Morphometry: implies the morphometric assessment of van Gieson stained sections, sections stained by immunohistology for  $\alpha$ -SMA and Iba-1, and sections stained with DAPI fluorescence.

<sup>C</sup>qPCR: implies quantitative reverse transcriptase PCR for the cytokines and remodeling enzymes listed in Table 2.

Abbreviations: F, female; IH, immunohistology; M, male; N, neutered; y, years.

**Supplemental Table S3.** Antibodies and immunohistological methods, with references for their use in canine tissues.

Antigen	Antibody (clone)	Source	Dilution	Pretreatment	Detection
Calprotectin <sup>6</sup>	Mouse mAb (MAC 387)	Neomarkers	1:700	EDTA	EnVision Mouse
CD3 <sup>10</sup>	Mouse mAb (F.7.2.38)	Dako	1:200	EDTA	EnVision Mouse
CD18 <sup>8</sup>	Mouse mAb (CA16.3C10)	LABL, Davis, CA, USA	1:25	Citrate	EnVision Mouse
CD20 <sup>2</sup>	Rabbit pAb	Thermo Scientific	1:1000	n/a	EnVision Rabbit
CD31 <sup>7</sup> (PECAM1)	Mouse mAb (JC70A)	Dako	1:20	EDTA	EnVision Mouse
Flk-1 <sup>11</sup> (VEGFR-2)	Mouse mAb (A-3)	Santa Cruz	1:50	EDTA	EnVision Mouse
Factor VIIIra <sup>1</sup>	Rabbit pAb	Dako	1:100	Citrate	EnVision Rabbit
MHC II, HLA-DR <sup>5</sup>	Mouse mAb (TAL 1B5)	Abcam	1:1500	Citrate	EnVision Mouse
Iba-1 <sup>4</sup>	Rabbit pAb	Wako	1:750	Citrate	EnVision Mouse
ICAM-1	Mouse mAb (CL18/1D8 or CL18/6)	M. Oyama <sup>A</sup>	1:300	Citrate	EnVision Mouse
$\alpha$ -SMA <sup>3</sup>	Mouse mAb (1A4)	Dako	1:400	n/a	Dako REAL



TGF- $\beta$ 1	Mouse mAb (TB21)	Acris	1:50	Citrate	Dako REAL
VEGF <sup>9</sup>	Goat pAb	Santa Cruz	1:50	EDTA	Goat HRP

<sup>A</sup>The antibody was kindly provided by Prof M. Oyama, Department of Clinical Studies, University of Pennsylvania, School of Veterinary Medicine.

Abbreviations:  $\alpha$ -SMA,  $\alpha$ -smooth muscle actin; CD, cluster of differentiation; citrate, citrate buffer pretreatment; EDTA, EDTA pretreatment; Factor VIIIra, factor VIII-related antigen; Flk-1, fetal liver kinase-1; HLA-DR, human leukocyte antigen – D related; HRP, horseradish peroxidase; Iba-1, ionized calcium binding adaptor molecule-1; ICAM-1, intracellular adhesion molecule-1; LABL, Leukocyte Antigen Biology Laboratory; mAb, monoclonal antibody; MHC, major histocompatibility complex; n/a, not applicable; pAb, polyclonal antibody; PECAM-1, platelet endothelial cell adhesion molecule-1; TGF- $\beta$ 1, transforming growth factor- $\beta$ 1; VEGF, vascular endothelial growth factor; VEGFR-2, vascular endothelial growth factor receptor-2.

1. Avallone G, Hembold P, Caniatti M, Stefanello D, Nayak R C; Roccabianca P. The Spectrum of Canine Cutaneous Perivascular Wall Tumors : Morphologic, Phenotypic and Clinical Characterization. *Vet Pathol.* 2007;44:607–620.

2. Brachelente C, Affolter VK, Fondati A, et al. CD3 and CD20 Coexpression in a Case of Canine Cutaneous Epitheliotropic T-Cell Lymphoma (Mycosis Fungoides). *Vet Pathol.* 2015;53:563–566.
3. Gofflot S, Kischel P, Thielen C, Radermacher V, Boniver J, de Leval L. Characterization of an antibody panel for immunohistochemical analysis of canine muscle cells. *Vet Immunol Immunopathol.* 2008;125:225–233.
4. Ide T, Uchida K, Kagawa Y, Suzuki K, Nakayama H. Pathological and immunohistochemical features of subdural histiocytic sarcomas in 15 dogs. *J Vet Diagnostic Investig.* 2011;23:127–132.
5. Kipar A, Baumgartner W, Vogl C, Gaedke K, Wellman M. Immunohistochemical Characterization of Inflammatory Cells In Brains of Dogs with Granulomatous Meningoencephalitis. *Vet Pathol.* 1998;35:43–52.
6. Kipar A, Baumgärtner W, Kremmer E, Frese K, Weiss E. Expression of major histocompatibility complex class II antigen in neoplastic cells of canine cutaneous histiocytoma. *Vet Immunol Immunopathol.* 1998;62:1–13.
7. Luong RH, Baer KE, Craft DM, Ettinger SN, Scase TJ BP. Prognostic significance of intratumoral microvessel density in canine soft tissue sarcomas. *Vet Pathol.* 2006;43:622–631.
8. Moore PF, Schrenzel MD, Affolter VK, Olivry T, Naydan D. Canine cutaneous histiocytoma is an epidermotropic Langerhans cell histiocytosis that expresses CD1 and specific beta 2-integrin molecules. *Am J Pathol.* 1996;148:1699–1708.

9. Stoica G, Lungu G, Martini-Stoica H, Waghela S, Levine J, Smith R. Identification of cancer stem cells in dog glioblastoma. *Vet Pathol.* 2009;46:391–406.
10. Vezzali E, Parodi AL, Marcato PS, Bettini G. Histopathologic classification of 171 cases of canine and feline non-Hodgkin lymphoma according to the WHO. *Vet Comp Oncol.* 2010;8:38–49.
11. Yonemaru K, Sakai H, Murakami M, Yanai T, Masegi T. Expression of Vascular Endothelial Growth Factor, Basic Fibroblast Growth Factor, and Their Receptors (Flt-1, Flk-1, and Flg-1) in Canine Vascular Tumors. *Vet Pathol.* 2006;980:971–980.

## **CURRICULUM VITAE**

First name Family name: Stefania Gasparini  
Date of birth: 02/07/1986  
Place of birth: Camposampiero (PD)  
Nationality: Italian

### **School education**

09/1992 – 06/1997 Scuola elementare I.C. Ardigò, Padova, Italy  
09/1997 - 06/2000 Scuola media Mameli, Padova, Italy  
09/2000 - 07/2005 Liceo Scientifico Ippolito Nievo, Padova, Italy

### **Highest school-leaving qualification**

07/2005 Liceo Scientifico Ippolito Nievo, Padova, Italy

### **Studies**

09/2006 – 10/2012 5-years Master's degree in Veterinary Medicine -  
Faculty of Veterinary Medicine of Padova, Agripolis,  
Viale dell'Università, 35020 Legnaro (PD) (Italy)

### **Veterinary medicine degree examination**

22/10/2012 Faculty of Veterinary Medicine of Padova, Agripolis,  
Viale dell'Università, 35020 Legnaro (PD) (Italy)

### **Preparation of the thesis**

09/2014 – 03/2019 Under the direction of Prof. Dr. med vet. Anja Kipar  
at the Institute of Veterinary Pathology  
of the Vetsuisse Faculty, University of Zurich  
Director Prof. Dr. med. vet. Anja Kipar  
09/2014-12/2016 Internship in Veterinary Pathology at the Institute of  
Veterinary Pathology of the Vetsuisse Faculty,  
University of Zurich

